ISPRS Journal of Photogrammetry and Remote Sensing 116 (2016) 42–54

Contents lists available at ScienceDirect

ISPRS Journal of Photogrammetry and Remote Sensing

journal homepage: www.elsevier.com/locate/isprsjprs

The variants of an LOD of a 3D building model and their influence on spatial analyses

Filip Biljecki [a,*], Hugo Ledoux [a], Jantien Stoter [a], George Vosselman [b]

[a] 3D Geoinformation Research Group, Delft University of Technology, Delft, The Netherlands
[b] Department of Earth Observation Science, Faculty of Geo-Information Science and Earth Observation—ITC, University of Twente, Enschede, The Netherlands

ARTICLE INFO

Article history:
Received 14 July 2015
Received in revised form 17 February 2016
Accepted 3 March 2016
Available online 21 March 2016

Keywords:
Geometric reference
3D GIS
LOD1
LOD2
CityGML

ABSTRACT

The level of detail (LOD) of a 3D city model indicates the model's grade and usability. However, there exist multiple valid variants of each LOD. As a consequence, the LOD concept is inconclusive as an instruction for the acquisition of 3D city models. For instance, the top surface of an LOD1 block model may be modelled at the eaves of a building or at its ridge height. Such variants, which we term geometric references, are often overlooked and are usually not documented in the metadata. Furthermore, the influence of a particular geometric reference on the performance of a spatial analysis is not known.

In response to this research gap, we investigate a variety of LOD1 and LOD2 geometric references that are commonly employed, and perform numerical experiments to investigate their relative difference when used as input for different spatial analyses. We consider three use cases (estimation of the area of the building envelope, building volume, and shadows cast by buildings), and compute the deviations in a Monte Carlo simulation.

The experiments, carried out with procedurally generated models, indicate that two 3D models representing the same building at the same LOD, but modelled according to different geometric references, may yield substantially different results when used in a spatial analysis. The outcome of our experiments also suggests that the geometric reference may have a bigger influence than the LOD, since an LOD1 with a specific geometric reference may yield a more accurate result than when using LOD2 models.

1. Introduction

One of the most important aspects when specifying the acquisition of 3D city models and describing the metadata of existing models is the level of detail (LOD), a concept that conveys the complexity of the models and their degree of abstraction from the real-world (Biljecki et al., 2014c). The most prominent LOD categorisation is the one found in the OGC standard CityGML (Open Geospatial Consortium, 2012; Gröger and Plümer, 2012; Kolbe, 2009), the international standard to store and exchange 3D city models, which we use in this paper.

Practitioners and researchers rely on the LOD concept to specify the fineness of the geometry of the models to be acquired. However, specification-wise the LOD is only one of the aspects to consider when acquiring 3D city models because from a geometric standpoint, there exist multiple variants of models within each LOD. For instance, an LOD1 block model (we define the LODs in Section 2) of a building may be modelled in a multitude of possibilities (Fig. 1): among other options, the top surface might represent the height at the eaves of a building or the height at the top of the construction. If we ignore the elevation, the footprint may be modelled at the position of the walls, or it may represent a projection of the roof edge polygon to the ground. This example already results in four variants of an LOD1 model, a fraction of all the possibilities, as we show in Section 3.

It is our experience that these modelling choices, which we describe as *geometric references*, are often overlooked by practitioners when acquiring, processing and utilising 3D city models. Furthermore, they are rarely documented in the metadata of the data set, usually because it is not possible to store such information, as in the case with CityGML. The awareness of the geometric reference is important because, as we show in Section 4, different geometric references within the same LOD may lead to considerable differences in the results of a spatial analysis. As a consequence of the ambiguous specifications, this may lead to errors in the utilisation of the models.

* Corresponding author at: 3D Geoinformation Research Group, Department of Urbanism, Faculty of Architecture and the Built Environment, Delft University of Technology, Julianalaan 134, 2628 BL Delft, The Netherlands.
E-mail addresses: f.biljecki@tudelft.nl (F. Biljecki), h.ledoux@tudelft.nl (H. Ledoux), j.e.stoter@tudelft.nl (J. Stoter), george.vosselman@utwente.nl (G. Vosselman).

http://dx.doi.org/10.1016/j.isprsjprs.2016.03.003
0924-2716/

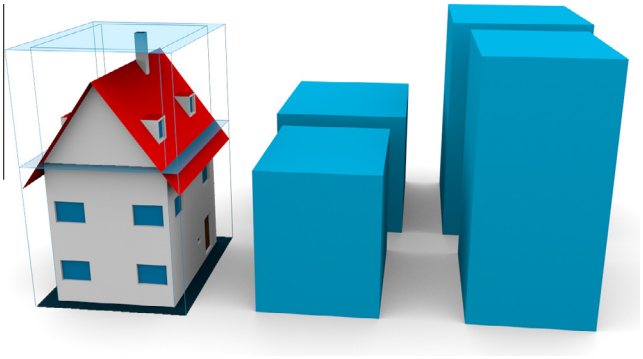

Fig. 1. Four variants (geometric references) of an LOD1 block model. The elevation of the top surface of a block model may be modelled at, among other options, at the eaves and at the top of the construction. Similarly, the footprint (and therefore the walls) may be modelled at the footprint or at the outline of the roof edges. Such combinations result in a multitude of modelling possibilities within the same LOD, which can cause errors in a spatial analysis if not documented properly.

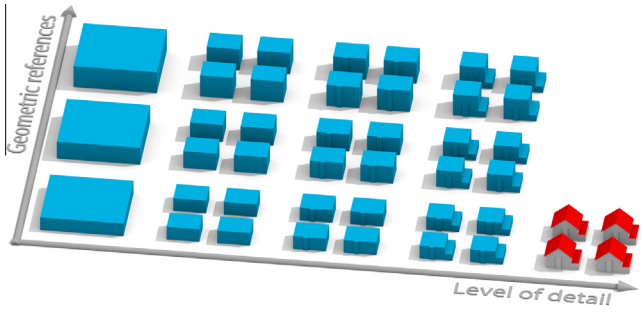

Fig. 2. The orthogonal relation between the LOD and geometric reference concepts. The image contains five LODs (four block models and a more detailed model). Within each of these LODs there exist multiple variants of geometric references. This example illustrates the different geometric references for the height of the block models (heights at the eaves, half of the height of the roof structure, and top height of the building). The figure is limited since it is only a subset of the possible LODs and GRs.

In this paper we provide an insight into this topic by covering the following aspects: we (1) derive an inventory of the most frequent geometric references, based on a survey of current practices of acquisition and modelling (Section 3); (2) run experiments with procedurally generated models in a Monte Carlo simulation and show that using models of the same LOD, but with different geometric references, potentially leads to substantially different results differing between use cases (Section 4). Our experiments and the underlying method can be used to determine the optimal specification suited for a specific use case of a 3D city model. Furthermore, we (3) propose a number of recommendations, such as an extension of the INSPIRE Building model standard (Section 5).

While we focus on CityGML, our work is applicable to any other 3D standard and LOD taxonomy, as we did not encounter any that regards geometric references.

2. Background and related work

We define a geometric reference as the modelling choice of the boundaries of the captured feature. This concept is orthogonal to the concept of LOD, since the LOD refers to the spatio-semantic richness of the representation (Stadler and Kolbe, 2007; Biljecki et al., 2014c). The relation between the LOD and geometric reference concepts is outlined in Fig. 2.

In this research, we focus on the two geometric references that, in our opinion, account for the majority of the ambiguities found in practice:

- *Vertical reference of the top surface of block models*: what does the elevation of the top surface of the block model represent. This is applicable to LOD1 models only.
- *Horizontal reference of the footprint*: what does the footprint (and the generated walls) represent. This is applicable to both LOD1 and LOD2 models, and to some extent to LOD3 models which are derived by supplementing LOD2 models with detailed façade geometry (Becker, 2009), and mixed-LOD models (Novaković, 2011; Franić et al., 2009; Arroyo Ohori et al., 2015a). This reference is also relevant in 2D GIS (maps), e.g. in ground plans containing 2D building footprints, which as well can be modelled according to multiple references.

2.1. Acquisition of LOD1 and LOD2 models and their ambiguities

In the standard CityGML, an LOD1 model is described as a block model with flat roof structure, and it is the coarsest volumetric representation that the standard contains. These models are frequently derived by extruding a footprint to a height derived in separate measurements (Ledoux and Meijers, 2011; Arroyo Ohori et al., 2015b), and are increasingly available as open data (Kolbe et al., 2015; Stoter et al., 2015). While LOD1 models are coarse, they may be very accurate and are used in a number of applications (van den Brink et al., 2013; Biljecki et al., 2015c), as they provide a favourable balance between simplicity and usability (Hofierka and Zlocha, 2012). For instance, they may be used in assessing the propagation of traffic noise (Czerwinski et al., 2007; Stoter et al., 2008; Ranjbar et al., 2012), in shadow analyses (Strzalka et al., 2012), and line of sight analyses (Yaagoubi et al., 2015).

An LOD2 model has generalised roof shapes (Kolbe, 2009; Gröger and Plümer, 2012). As a result, and owing to the practice that their walls are frequently derived as projections from roof edges, LOD2 models usually do not contain explicitly modelled roof overhangs. Thanks to the increased detail over LOD1 models, they are used for a larger number of purposes, for instance, in the determination of the usable space of a building (Boeters et al., 2015), improvement of satellite positioning (Wang et al., 2013), and in the estimation of the solar irradiation of the rooftops (Biljecki et al., 2015a).

The reason for the existence of the multiple geometric references lies in the lineage: the different workflows and approaches for acquiring 3D city models. This is especially the case for LOD1 and LOD2 which are largely derived automatically or semi-automatically with a number of different techniques (see Haala and Kada (2010), Tomljenovic et al. (2015), Musialski et al. (2013), Verdie et al. (2015) for overviews).

Fig. 3 clarifies this diversity by showing some of the general scenarios to derive LOD1 and LOD2 models: (left) the acquisition with airborne techniques, (right) with terrestrial observations coupled with the information about the height, and (centre) the scenario of the combination of the airborne and terrestrial measurements.

Airborne techniques (airborne laser scanning—ALS, and photogrammetry) are frequently employed for deriving LOD1 and LOD2 models (e.g. see the work of Suveg and Vosselman (2004), Xiong et al. (2015), Rottensteiner (2003), Sirmacek et al. (2012), and Demir and Baltsavias (2012)). These techniques generally involve the acquisition of the roof surface, and subsequently the projection of its edges to the ground to derive the walls and the footprint. This inherently causes buildings to be wider than they are in reality. In such a scenario, LOD1 models are usually derived by constructing a horizontal plane at an elevation such as roof edges or roof ridges, and LOD2 models do not contain differentiated roof overhangs—they are part of the (combined) geometry of the roof.

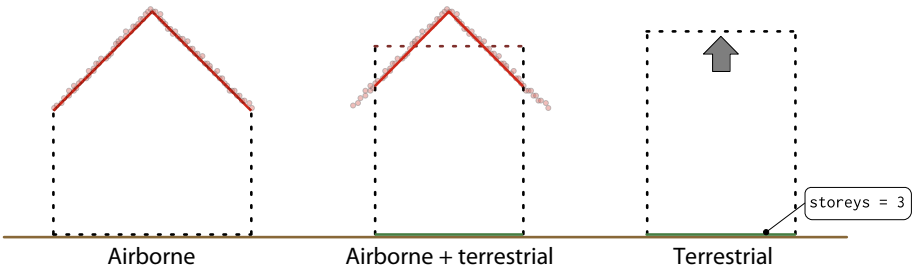

Fig. 3. Some of the common acquisition workflows accounting for the vast majority of sources of LOD1 and LOD2 models, resulting in different geometric references.

When airborne techniques are supplemented with terrestrial measurements, such as a geodetic survey (centre example), the footprint and walls are at their *actual* position. Their location also serves as a *constraint* for the reconstruction of the models. For instance, in case of ALS, only points with planar coordinates within the footprint are considered in the reconstruction of a building. This means that in the reconstruction of the LOD2 model the roof surface may be smaller with the roof edges reduced, since the area representing the roof overhangs is usually not included, as it is constrained by the footprint polygon. When producing LOD1 models, the elevation of the top surface is commonly derived from a statistical analysis of the LiDAR data, such as the median or average of the heights of all points within the footprint. Both the LOD1 and the LOD2 models are shown in the centre example.

Finally, the example on the right indicates the extrusion from 2D footprints in combination with various forms of attribute data, such as the number of floors (Over et al., 2010; Goetz, 2013; Coors, 2003), or a building height derived in cadastral measurements, e.g. height at the eaves (Aringer and Roschlaub, 2014; He et al., 2012a).

A prominent technique of deriving LOD1 and LOD2 models, that is outside this observational context, is generalisation from existing models of finer LODs (Diakité et al., 2014; El-Mekawy et al., 2011; Mao et al., 2012; Forberg, 2007; Zhao et al., 2012; Li et al., 2013). In the same way, most papers on generalisation do not specify the horizontal and vertical reference of the generalised models.

2.2. Related work

The INSPIRE Building model is a relevant source on this subject, as it provides metadata to express the references in 3D city models, and we cover the document in Section 3.1.

The research of Biljecki et al. (2014b) investigates what are the possible heights of the LOD1 top surface. We extend the work by involving more vertical references, cover the horizontal references (footprint), include LOD2 models, and take into account multiple spatial analyses.

Brasebin et al. (2012) partially investigated this problem. They term the different horizontal references as *modelling choices* and estimate the influence of two references on the estimation of the sky view factor—the degree to which the sky is obscured by surrounding buildings (Johnson and Watson, 1984).

Sargent et al. (2015) point out that different users prefer different height values of buildings in 2D topographic databases, and recommend that national mapping agencies should provide more than one building height value. The values are termed as *building height characteristics*.

Pedrinis and Gesquière (2016) acknowledge multiple forms of footprints as *inconsistencies*, and deem them inconvenient when matching data sets from multiple databases. In their work they present a remedy for correcting the offset between two data sources caused by different geometric references, to allow their merging.

Oude Elberink (2008) recognised the problem of the ambiguity of the uncertain reference of the footprint when reconstructing the LOD2 models from point clouds in conjunction with 2D data. The research does not further investigate this topic, but it is important to mention as one of the first sources we have found that indicates the implications of unknown geometric references, e.g. in the combination of multiple geo-data sources to produce models of unknown lineage.

2.3. Refinement of LODs

Considering that the geometric references are related to the concept of LOD, it is important to consider the related work in LOD definitions.

There have been recent efforts such as Benner et al. (2013), Löwner et al. (2013), and Biljecki et al. (2016) to redefine the well-known CityGML LODs to cope with the increasing number of acquisition techniques, ambiguities, and use cases. As a result, Biljecki et al. (2016) have extended the *traditional* LODs of CityGML to reflect the actual acquisition practices and to provide the industry with a more precise scheme to express the LOD of a 3D city model. They have refined the LOD1 and LOD2 models into four sub-LODs in each group. The previously introduced Fig. 2 also illustrates an example for this context: the first four LODs are variants of LOD1 models which increase in their complexity: LOD1.0 contains aggregated buildings, LOD1.1 mandates individual buildings, LOD1.2 is derived from fine footprints, and in LOD1.3 the extruded block model may have multiple heights.

We regard the improved specification as follows. First, the geometric references that we investigate are applicable to the refined LODs, however, in the experiments we focus the most common LOD1 and LOD2 models available in practice (LOD1.2—individual buildings of a fine footprint extruded to a single height, and LOD2.1—simple LOD2 models without roof overhangs). In Fig. 4 we show the relation between the two concepts. Their specification refines the standard LODs into 16 refined LODs. Each of these may be modelled according to several different geometric references (e.g. $LOD1.2^{GR1}$, $LOD1.2^{GR2}$, etc.), resulting in a large number of different representations.

Second, the refined specification differentiates a finer version of the LOD2 model, specified as LOD2.3, that is acquired as a combination of terrestrial and airborne techniques (centre case shown in Fig. 3), where the roof overhangs are explicitly modelled. Such models are not common in practice, but they are of higher quality and they diminish deviations from the real-world since both the footprint and roof edges are at their actual location. We include this LOD2 variant in our experiments (Section 4) and investigate the relative difference between it and its coarser LOD2 counterpart across different geometric references.

3. Inventory of the references in LOD1 and LOD2

3.1. The INSPIRE Building model

The INSPIRE Data Specification for the spatial data theme Building (INSPIRE Thematic Working Group Buildings, 2013; Gröger and

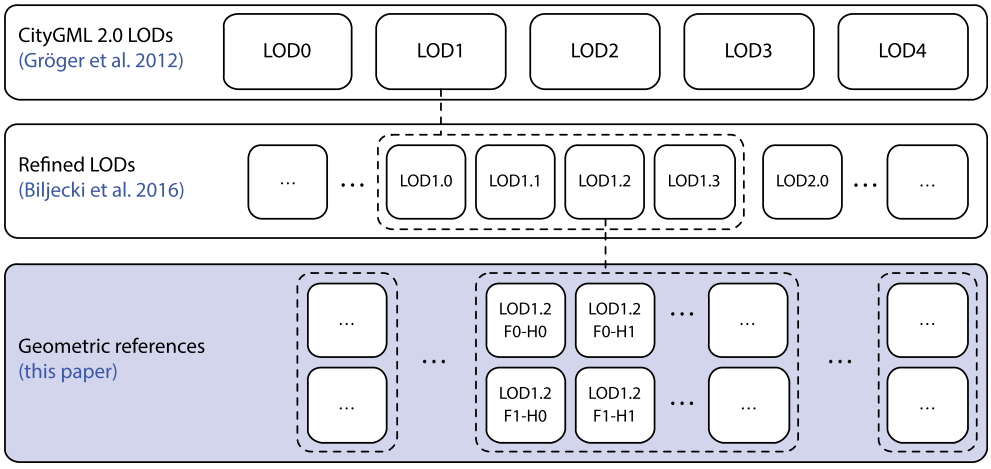

Fig. 4. The relation of our research and LOD research efforts. Our work extends the refined LOD specification by describing multiple variants of each LOD, resulting in dozens of combinations. The shorthands will be explained thorough the text.

Plümer, 2013) covers 2D and 3D representations, and focuses on the footprint and elevation in the context of buildings, representing a solid foundation for this paper.

The specifications mandate that the horizontal and vertical levels of a building that was chosen to represent its footprint and elevation have to be documented. It presents a code list and definition of a number of references of buildings in LOD1 and LOD2, that are intended both as descriptors of the geometric representation and attributes (e.g. in 2D data). These references are represented by a value type `horizontalGeometryReference` or `ElevationReferenceValue`, i.e. a list of self-explanatory elements considered to capture a horizontal or vertical geometry.

For the vertical reference (elevation of the top surface of the LOD1 block model), this is realised through the attribute `verticalGeometryReference3DTop`, and a value from the corresponding code list `ElevationReferenceValue`, such as `topOfConstruction`. The list is extensive as it takes into account uncommon cases, for instance, the case where the height of the eaves is not equal (e.g. the eaves on one side of the building are higher than the eaves on the other side). At the same time, the standard contains the value `generalRoof`, which is ambiguous considering that it may refer to any point on the roof.

While the standard recommends a number of references for the top surface in LOD1, as we show in Section 3.2, this list is not complete. For instance, another relevant value may be the highest point of a building (not to be confused with `topOfConstruction`), a height level that includes above-roof elements such as chimney and antennas, and that is frequent in generalisation, where the coarse models are sometimes constructed as bounding boxes capturing the extent of a building. This level is a possible value in the code list `ElevationReferenceValue` as `highestPoint`, but for some reason it is not listed as a recommended value for `verticalGeometryReference3DTop`.

The second relevant concept is the footprint, which is also covered by the INSPIRE Building model. The reference for the geometry of the footprint is expressed through the `HorizontalGeometryReferenceValue`, with possible values such as `footPrint` and `roofEdge`. This reference is applicable to both LOD1 and LOD2.

3.2. A survey of geometric references in practice

We have made a survey of current practices of horizontal and vertical references in LOD1 and LOD2 through an extensive review of research papers that deal with the acquisition of 3D city models, by contacting acquisition companies, and by investigating the specifications of national mapping agencies (NMAs).

An overview of research papers such as Mao et al. (2012), He et al. (2012b, 2013), Guercke et al. (2011), Diakité et al. (2014), Commandeur (2012), Oude Elberink et al. (2013), Hermosilla et al. (2012), Schwalbe et al. (2005), Zhang et al. (2006), Brasebin et al. (2016) yielded an extensive overview of the references, but also strengthened our impression that the majority of research papers that describe methods to acquire buildings do not explicitly elaborate on the employed geometric reference.

The specifications of local governments and national mapping agencies contained some information about the geometric references. We have obtained them through publicly published specifications of data or tenders (e.g. Netherlands—Stoter et al. (2014), UK—Ordnance Survey (2014) and Sargent et al. (2015), Germany—AdV (2011, 2013), Aringer and Roschlaub (2014), and Switzerland—SwissTopo (2010)), and through our involvement in the EuroSDR 3D Special Interest Group (Stoter et al., 2015).

Most of the references that we have found are standardised by the INSPIRE Building model (Section 3.1). However, while INSPIRE provides a sizeable list of vertical and horizontal geometric references, we have discovered that there are additional values occurring in practice, rendering the standard incomplete. We list these below.

3.3. Vertical geometric references (top of the LOD1 block model)

Our survey has shown that the height of the top surface of the LOD1 block model may be modelled at a multitude of elevations. We list and describe them in details, and group them into three categories. For each height reference we assign an internal shorthand for easier referencing in the continuation of the paper, and in Table 1 we give an overview with a relation to the INSPIRE Building model where possible. Table 1 also shows that the INSPIRE Building model does not cover all references, hence this inventory can be seen as possible extension of the standard (this is elaborated in Section 5).

3.3.1. References related to the roof structure

As indicated in Section 2.1, the vertical geometric references are mostly related to the roof structure, and this category accounts for most of the specifications observed in the survey. For instance, in photogrammetry the height of LOD1 models is usually taken from the roof edges or at the ridge of the roof.

Table 1
List of vertical geometric references (representations for the height of the top surface of the LOD1 block model). The equal sign means that the reference is re-used from INSPIRE. The asterisk (*) indicates that `generalRoof` could correspond in most of the cases, but not always (especially in the case of flat roofs).

Code (Section 3.3)	Height at	INSPIRE ref.	Our ref.
H0	Roof edges	`generalRoofEdge`	=
H1	Roof eaves	`generalEave`	=
H2	One third of the roof height	`generalRoof`	`oneThirdRoof`
H3	Half of the roof height	`generalRoof`	`halfRoof`
H4	Two thirds of the roof height	`generalRoof`	`twoThirdRoof`
H5	Top of the roof (i.e. ridge)	`topOfConstruction`	=
H6	Highest point of the building	`highestPoint`	=
HL-avg	Average height of the point cloud	*	`avgHeightLiDAR`
HL-med	Median height of the point cloud	*	`medHeightLiDAR`
HL-max	Maximum height of the point cloud	*	`maxHeightLiDAR`
Hx	Varies. E.g. $f \times h$	N/A	`NonEleAtt`

H0 Height at the roof edges. Because of the roof overhangs, roof edges may have an elevation that is lower than the one of the highest point of the walls, hence this is the lowest point of the roof structure, and therefore the lowest possible reference of the top surface.

H1 Height at the roof eaves (the intersection of the roof and the wall plane; see Fig. 1). This value is common in terrestrial measurements, and it is usually not visible for airborne techniques. It corresponds to the reference H0 in the case when there are no roof overhangs.

H2 Height at one third of the height of the roof structure (with H0 as the lowest point of the roof structure).

H3 Height at half of the height of the roof structure.

H4 Height at two thirds of the height of the roof structure.

H5 Height at the top of the roof (top ridge). This is a value typical in the generalisation from models with a finer LOD. It can also be derived from point clouds.

H6 Height at the top of the construction of the building. This value encompasses the whole construction (similar to a bounding box), and it is usually used with generalisation from LOD3 where antennas and chimneys are available. In case there are no such structures that extend beyond the top of the roof, the value corresponds to H5.

3.3.2. References based on the statistics of a point cloud

Many LOD1 models are derived from airborne LiDAR data by extruding the footprint to a certain height derived from the points whose projection is within the footprint of the building (see the central scenario in Fig. 3). Some of these references overlap with certain references in the previous category, however, a norm is to take the average or the median height of all points within a footprint (Arefi et al., 2008; Stoter et al., 2014).

This approach is ambiguous and it depends on the characteristics of the ALS survey, and the reflection properties of the various roof surfaces of a building. For instance, due to the relative position of the aircraft, in one occasion the point cloud of a building may contain only points that represent the roof. However, in another survey the point cloud of the same building may contain lots of points representing walls (if not filtered), essentially resulting in a different elevation of the median of the heights and other similar statistically derived heights from a point cloud

HL-avg Height derived from the average of the heights in a LiDAR point cloud. For buildings with sloped roof in practice it is usually between H2 and H4, however, for flat roofs without roof structures it may be below the elevation of the roof due to points on walls if not filtered.

HL-med Height derived from the median of the heights in a LiDAR point cloud, favoured over the average to filter outliers. In practice it is usually between H2 and H4, however, for flat roofs it may also be below H0 if points on the wall are not filtered.

HL-max Height of the highest elevation in the point cloud. If there is no vegetation, usually it corresponds to H6.

3.3.3. Non-elevation attribute references

We have encountered a number of 3D city models obtained with the extrusion of footprints to an elevation that is available as an *indirectly derived* attribute such as the number of floors (Over et al., 2010; Goetz, 2013; Coors, 2003). Such attributes are not overly reliable for determining the height of a building, but nevertheless they are not uncommon as they provide an approximate height that may be sufficient for visualisation and similar purposes (Glander and Döllner, 2009; Kwan, 2000). We jointly refer to this reference as:

Hx Height derived from non-elevation data, such as the number of floors (e.g. number of floors f multiplied by an assumed floor height h).

3.4. Horizontal geometric references (footprint of LOD1 and LOD2 models)

The list of horizontal geometric references is shorter, and it is closely related to the used acquisition technique. The two main references (accounting for virtually all models we have found) are:

F0 The footprint is modelled at its actual location. This reference is typical for terrestrial measurements, and it corresponds to the INSPIRE reference `footprint`.

F1 The footprint is derived as a projection of the roof edges of the building. In case there are no roof overhangs it corresponds to F0. How much a model with F1 deviates from the reality essentially depends on the length of the roof overhangs. INSPIRE labels this reference as `roofedge`.

In Oude Elberink (2010) and Schwalbe et al. (2005) we have encountered an *artificial* reference that is derived by offsetting the F1 footprint by a fixed length to "compensate" for the roof overhangs to produce models that attempt to resemble closer the reality. Such reference applies to LOD2.1 models—the measured roof edge is truncated by a distance d, and to LOD2.3—the walls are offset by a distance d, preserving the roof edges, and resulting in a LOD2 model with explicitly modelled roof overhangs of a predetermined fixed distance. In areas where buildings with overhangs are predominant and the value of d is close to the average size, such straightforward practice may provide models of a higher quality.

Table 2
List of horizontal geometric references (the footprint of LOD1 and LOD2 models). The equal sign means that the reference is re-used from INSPIRE.

Code (Section 3.4)	Footprint at	INSPIRE ref.	Our ref.
F0	Actual location	`footprint`	=
Fd	Roof edges offset by a fixed distance	N/A	`offsetRoofEdge`
F1	Roof edges	`roofedge`	=

We use the code **Fd** to describe this reference, and in our experiments we use the value $d = 20$ cm as in Oude Elberink (2010). It is important to note that this transformation is employed on all buildings, including the ones with no overhangs, potentially resulting in a smaller footprint than it is in reality. This reference is not discussed in the INSPIRE Building model.

On top of these three references, which in our experience cover all the models found in practice, the INSPIRE Building model defines three additional references `aboveGroundEnvelope`, `envelope`, and `lowestFloorAboveGround`, which define footprints for special cases of buildings and models, such as taking into account the underground structure when it is larger than the horizontal extent of the building above the surface. Because we have not encountered such cases in practice, we do not include them in our work.

Similarly as in the previous table, in Table 2 we give the list of horizontal references for the footprint of a building.

4. Influence of the geometric references on a spatial analysis

It is *a priori* obvious that utilising models with different geometric references may result in substantial deviations in spatial analyses sensitive to the geometry, such as computing the volume of buildings and estimating their shadows. On the other hand, in some spatial analyses, such as the estimation of flooding, different geometric variants might not have a significant impact.

The goal of the experiments is to investigate numerically the differences between models of different geometric references when employed in a spatial analysis, and to obtain insights how geometric references affect the outcome of a particular spatial analysis. We perform a Monte Carlo simulation on a large set of procedurally generated buildings that we have adapted for this project, and we run the models through three spatial analyses to determine the deviation of each representation. Because each building is different, it has a different influence on such analysis, hence experiments need to consider a large number of dissimilar buildings. For instance, an LOD1 with the reference H6 is different in the case of a building with a chimney, and another building of the same dimensions without a chimney.

4.1. Methodology

Our method consists of three steps, which are explained below in more detail.

1. *Data acquisition: Procedural modelling of buildings and realisation of 3D models with multiple geometric references.*
   In the first step we generate a large number n of different 3D building models. For this purpose we use the CityGML procedural modelling engine Random3Dcity developed by Biljecki et al. (2014a), which we have extended to produce 3D city models in several geometric references according to the descriptions presented in Section 3. The engine first generates a large number of different buildings in a parametric form to take into account a large number of dissimilar scenarios, according to a customised shape grammar that resembles a specific real-world setting. The shape grammar has been adjusted to produce buildings that are predominant in Europe, and the values of building parameters (e.g. building height) have been sampled from a uniform distribution function according to the range of most residential buildings. Afterwards, the engine realises the models in CityGML in multiple LODs and in multiple geometric references. We use procedurally generated models because in practice it is difficult to obtain data in more than one representation (Biljecki et al., 2015b). Simulated GIS data has been used previously in research, primarily in experiments to assess uncertainty in spatial analyses (Li et al., 2000; Burnicki et al., 2007). Furthermore, such models provide an unlimited source of diverse data, the ground truth is known, and they are not burdened with acquisition errors. In real-world data it would be difficult to isolate the deviations caused by acquisition errors, and the ones induced by the different geometric references.
   Fig. 5 demonstrates an example of one building generated with the procedural modelling engine with the considered representations. Observe the two variants of LOD2: the LOD2.1, and LOD2.3 with the explicitly available roof overhangs. In the latter, the roof edge is always represented at its actual location, but the body of the building varies.
2. *Data utilisation: Performing a spatial analysis of the different representations.*
   In order to estimate the influence of the different specifications, we use each model as an input of a spatial analysis. For this task it is required to have a spatial analysis that results in unambiguously quantifiable results, hence, applications such as navigation and urban planning are excluded.
   Each representation r_i of a building b is used in a spatial analysis A producing a result $R = A^b_{r_i}$. For each building, also its ground truth $GT = A^b_{gt}$ is computed, which is known because the models are procedurally generated.

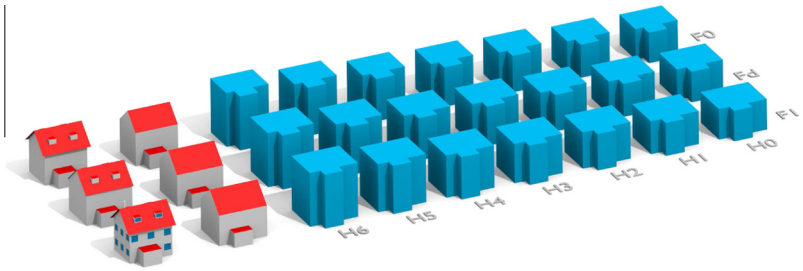

Fig. 5. An example of a building modelled in 27 representations. The blue block models are 21 variants of LOD1 (3 horizontal references × 7 vertical references). The three models lined next to the LOD1 group are three variants of LOD2.1 models, differentiated by the horizontal reference. The two models top left are LOD2.3 with references F0 and Fd (LOD2.3 with F1 is not possible). The bottom left is the LOD3 model for orientation. (For interpretation of the references to color in this figure legend, the reader is referred to the web version of this article.)

3. *Evaluation of the deviations.*
In this step we compare the different results and compute the errors for each LOD/GR combination. For each building b, and for each of the used representations r_i, the error in the result of a spatial analysis A is calculated as

$$\epsilon(A)^b_{r_i} = R - GT = A^b_{r_i} - A^b_{gt}$$

To put this residual in perspective, we also calculate the relative error

$$\rho(A)^b_{r_i} = \frac{R - GT}{GT} = \frac{\epsilon(A)^b_{r_i}}{A^b_{gt}}$$

Afterwards, for each of the representations the root mean square error (RMSE) values are derived:

$$\mathrm{RMSE}_{\epsilon(A)_r} = \sqrt{\frac{\sum_{b=1}^{n}\left(\epsilon(A)^b_r\right)^2}{n}} \quad \mathrm{RMSE}_{\rho(A)_r} = \sqrt{\frac{\sum_{b=1}^{n}\left(\rho(A)^b_r\right)^2}{n}}$$

where n is the number of buildings.

4.2. Investigated spatial analyses

In order to benchmark the different geometric references in a spatial analysis, and to investigate the relative differences in the results between multiple analyses, we have selected three use cases of 3D city models described below.

4.2.1. Analysis 1: Area of the building envelope

The information of the building envelope provides valuable input in several applications, and 3D city models are frequently used for this purpose. For instance, in assessing the cost of energy-efficient retrofitting of a building (Nouvel et al., 2013; Previtali et al., 2014), estimating the loss of energy in households (Kaden and Kolbe, 2013, 2014; Eicker et al., 2014), estimating indoor thermal comfort (Chwieduk, 2009), predicting cooling requirements (Perez et al., 2013), thermal simulations involving computational fluid dynamics (Hsieh et al., 2011; Maragkogiannis et al., 2014), analysing the urban heat island effect (van der Hoeven and Wandl, 2015), and in urban design evaluation (Yang et al., 2007).

The area of the building envelope is calculated as the sum of areas that comprise the shell of a building. We have implemented a software prototype that calculates the area from CityGML models.

4.2.2. Analysis 2: Volume of the building

Estimating the volume of a building has gained substantial attention in 3D GIS (Steuer et al., 2015; Biljecki et al., 2014a), and nowadays it is essential in use cases such as energy demand estimation (Bahu et al., 2015; Kaden and Kolbe, 2014; Strzalka et al., 2010, 2011), determination of property taxes (Boeters et al., 2015), estimation of the population in a given area (Gröger and Plümer, 2013; Sridharan and Qiu, 2013; Dong et al., 2010; Ural et al., 2011; Lwin and Murayama, 2009), urban planning (Ahmed and Sekar, 2015), material flow modelling and quantification of development densities (Meinel et al., 2009), and in the volumetric visibility analysis of urban environments (Fisher-Gewirtzman et al., 2013).

We have computed the volume of building solids (in m^3) with the Feature Manipulation Engine (FME[1]), automated by an iterating Python script. Because the volume calculated from the exterior shell systematically deviates from the volume of the interior, we follow the practice of Kaden and Kolbe (2014) who reduce the calculated volume by 25% to offset for the thickness of the walls and joists.

4.2.3. Analysis 3: Shadow casted by a building

The estimation of shadows cast by buildings and other urban features is a spatial analysis important for several use cases. For instance, the information of the shadow is used in the estimation of the insolation of buildings to account for the reduced yield for photovoltaic (PV) panels (Strzalka et al., 2012; Alam et al., 2013; Nguyen and Pearce, 2012; Fogl and Moudrý, 2016), in urban planning (Herbert and Chen, 2015), in determining the solar access of buildings (Morello and Ratti, 2009), in mass valuation of real estate (Helbich et al., 2013), and in developing strategies to mitigate heat (Bajsanski et al., 2016).

We have implemented a software prototype that estimates the area of the shadow cast by a building on the ground, for several positions of the sun.

4.3. Experiments and discussion

We have generated $n = 40,000$ buildings in 27 representations resulting in 1.1 M CityGML models. The relatively high value n was selected in order to have a large number of diverse configurations of buildings. A visual excerpt of the generated models is illustrated in Fig. 6.

Because of complex computations, in the third experiment (shadows) we use a subset of 400 buildings. However, due to the large number of measurements (for many different positions of the sun) we obtain a number of samples comparable to the number of samples available in the first two experiments.

The results of the three experiments are provided numerically in Table 3. In the following sections we compare the distribution of errors for a better understanding of the deviations, and discuss the results. In order to directly compare the differences between spatial analyses, in the table we present the relative errors.

4.3.1. Results of experiment 1 (envelope)

Fig. 7 shows the distribution of error of estimating the area of the building envelope. We observe from the results that there is a substantial difference between geometric references, and that the errors between references within the same LOD are not simply shifted—each distribution is unique, and it does not correspond to any known probability distribution. Some of the errors are gross (e.g. an error of 26% in case of LOD1-H6-F1), rendering models of this reference unusable for this purpose.

The peaks at 0 are from buildings with flat roofs without roof overhangs, where different geometric references do not have a significant influence.

Within LOD1 the RMSE ranges from 7% to 26%, while in LOD2 from <1% to 12%.

Our experiments show that for LOD1 the most suitable geometric reference is the combination of F0 and H4, and for LOD2 a model with the footprint at its actual location (F0). The Fd reference seems to be somewhat advantageous over F1. A paradoxical observation is that some combinations of references show that a coarser LOD can be more accurate than a finer LOD (e.g. LOD1-H3-F0 has a smaller RMSE than LOD2.1-F1).

LOD2.3 models with the footprint at F0 appear to provide an advantage over LOD2.1 models with the same reference, due to the more factual representation of the roof.

4.3.2. Results of experiment 2 (volume)

The distribution of errors in the second experiment is given in Fig. 8. We notice that the results are pronouncedly different from the first experiment, affirming that it is important to run these experiments for multiple different spatial analyses. In LOD1, the

[1] https://www.safe.com/fme.

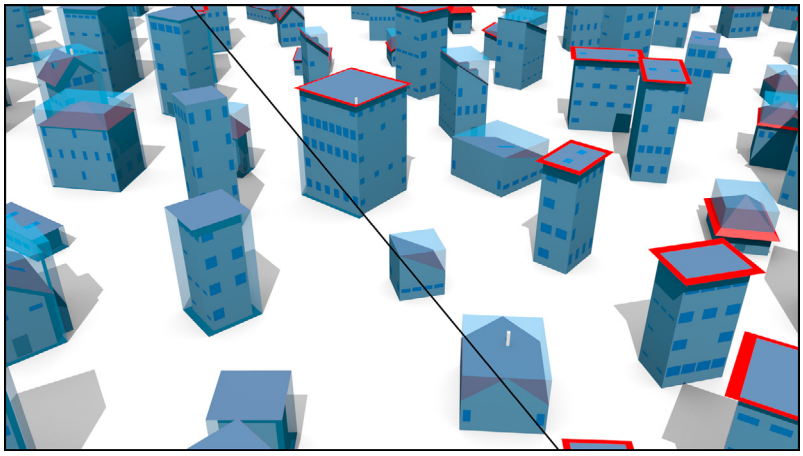

Fig. 6. A composite rendering of three subsets of our procedurally generated data sets: two LOD1 models with different footprint references separated by the thick black diagonal (LOD1-H5-F1, left of the diagonal, and LOD1-H5-F0, right), superimposed on an LOD3 model. Note that where the building has no overhangs the models correspond. Observe that some of the LOD1 models deviate more than the others depending on their configuration (e.g. compare the building on the far left with the garage in comparison with a building that has a flat roof and no overhangs).

Table 3
The relative RMSEs, expressed in percents, of the three analyses by the LOD and geometric references. The coloured markers indicate the magnitude of the error.

	Experiment 1			Experiment 2			Experiment 3		
	F0	Fd	F1	F0	Fd	F1	F0	Fd	F1
LOD1 H0	18	15	14	22	28	34	21	19	17
LOD1 H1	14	12	13	18	27	36	19	16	16
LOD1 H2	10	9	12	13	26	36	15	13	14
LOD1 H3	8	9	14	9	27	39	15	14	16
LOD1 H4	7	11	17	9	31	44	16	16	20
LOD1 H5	12	19	26	16	40	56	22	25	30
LOD1 H6	13	19	26	17	41	56	23	26	31
LOD2.1	7	8	12	10	27	38	14	12	13
LOD2.3	0	9		10	27		1	10	

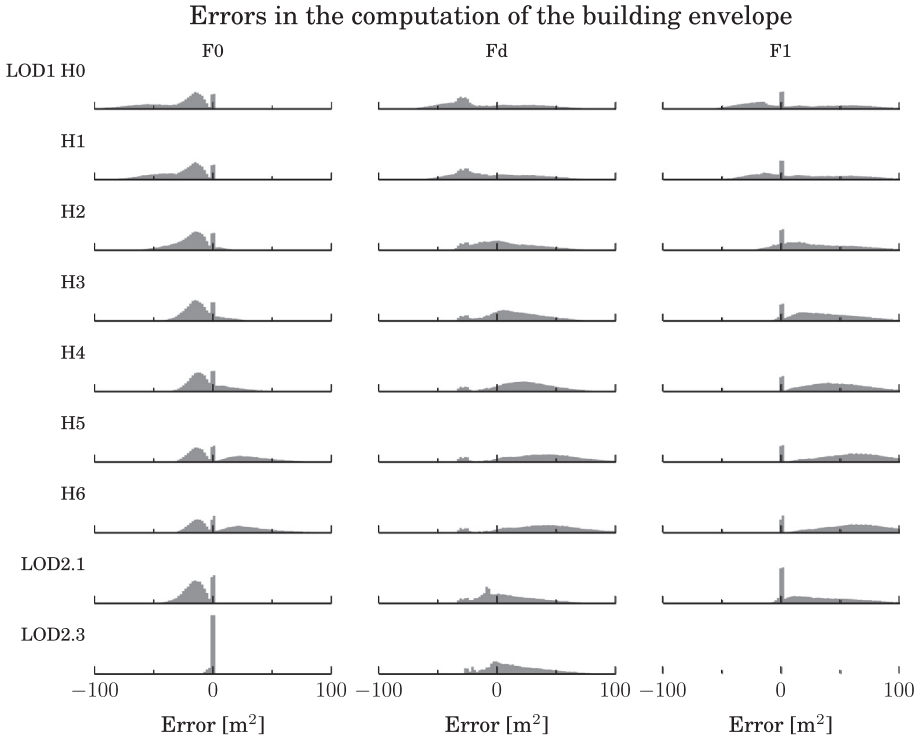

Fig. 7. Results of the first experiment involving the computation of the area of the building envelope.

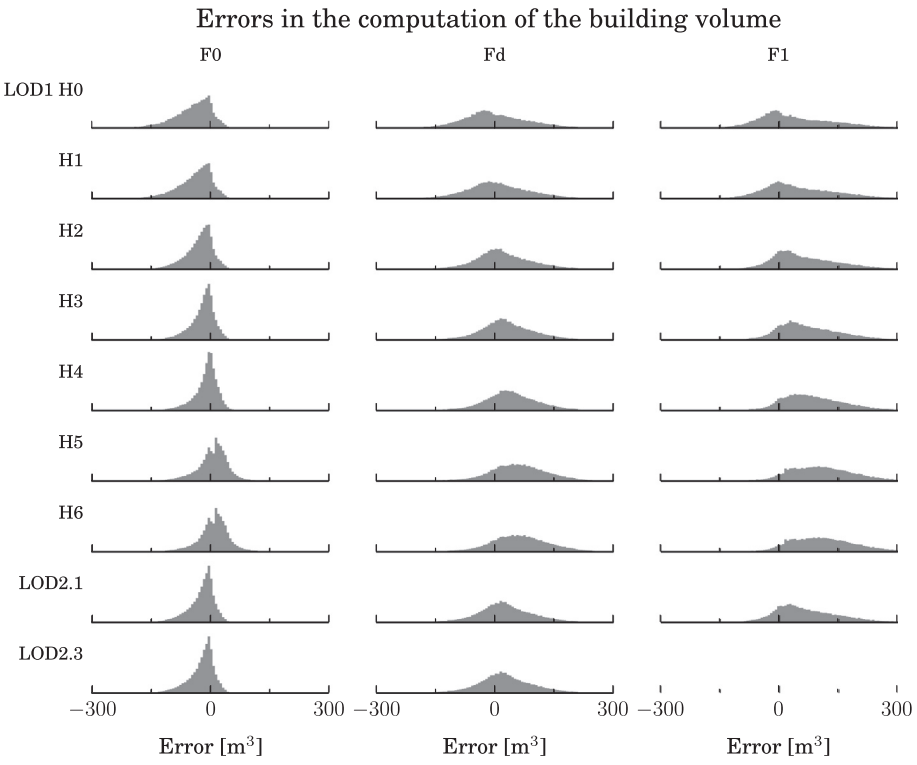

Fig. 8. Results of the second experiment involving the computation of the building volume.

errors range from 9% to 56%, and in LOD2 from 10% to 38%. Again, there is a substantial number of samples for which the error is small (peaks at zero), due to a number of building configurations which do not differ much among different geometric references.

The experiments suggest that the optimal representation appear to include models with a horizontal reference F0, due to the more truthful representation of the building body. Furthermore, the experiments show that LOD1 models may be fairly accurate in the computation of the volume if their top surface is modelled at the half of the roof structure.

In this analysis, however, LOD2.3 models do not seem to provide an advantage over LOD2.1 models, since the roof overhangs are not included in the computation of the volume, and therefore their presence provides no advantage here.

4.3.3. Results of experiment 3 (shadow)

The results of the third experiment are shown in Fig. 9. They also show that different geometric references have a substantial influence on this spatial analysis. Buildings with the footprint modelled at its actual location (F0) generally provide a more accurate analysis. LOD2.3 is more accurate than LOD2.1 when used for this purpose, since roof overhangs and dormers are present.

The range of errors in LOD1 is from 13% to 31%, while in LOD2 the errors range from 1% to 14%.

4.3.4. Conclusions from the experiments

Our experiments show that models of different geometric references have a significantly different effect when used in a spatial analysis. For instance, the range of errors is different between spatial analyses (cf. 9–56% and 1–31%, for the second and third experiment, respectively), hence different spatial analyses exhibit different sensitivity by using different GRs.

The work therefore proves the importance of considering the geometric reference when acquiring and utilising 3D city models. The relative differences between the results of spatial operations utilising models of the same LOD but of different geometric references may be gross. The most important conclusions are:

1. We show that because each spatial analysis has different requirements there is no optimal geometric reference. Our approach can be used to determine the most suitable geometric reference for a specific spatial analysis.
2. An interesting observation is that an LOD1 with a specific geometric reference may yield more accurate results than an LOD2 for some spatial analyses.
3. The results of the three spatial analyses indicate that the effect of the geometric references strongly depends on the configuration of the building. For instance, models of buildings with flat roofs and no roof overhangs are invariant across multiple LODs and geometric references. This is in contrast with buildings with a more complex configuration, such as the ones that contain non-flat roofs, and protrusions such as balconies, garages, and alcoves. We would expect that in other geographic areas, e.g. those with larger buildings and of different shape, the errors would be of different magnitudes. For future work it would be interesting to investigate the relation between the input distribution and the systematic error of the spatial analyses.
4. To some extent, the Fd reference seems to be advantageous over F1, however, it does more harm than good for buildings without overhangs or with overhangs that are shorter than the distance *d*. This is also visible in the histograms in the absence of peaks at 0.
5. The distribution of errors is not simply shifted between geometric references: it is unique for each geometric reference. This is caused by differences in the configurations of buildings.

These findings suggest that it is important to carry out such experiments for each spatial analysis to understand the different behaviour of the specifications, but several can be built upon these, so could be reused to quickly consider a new use case.

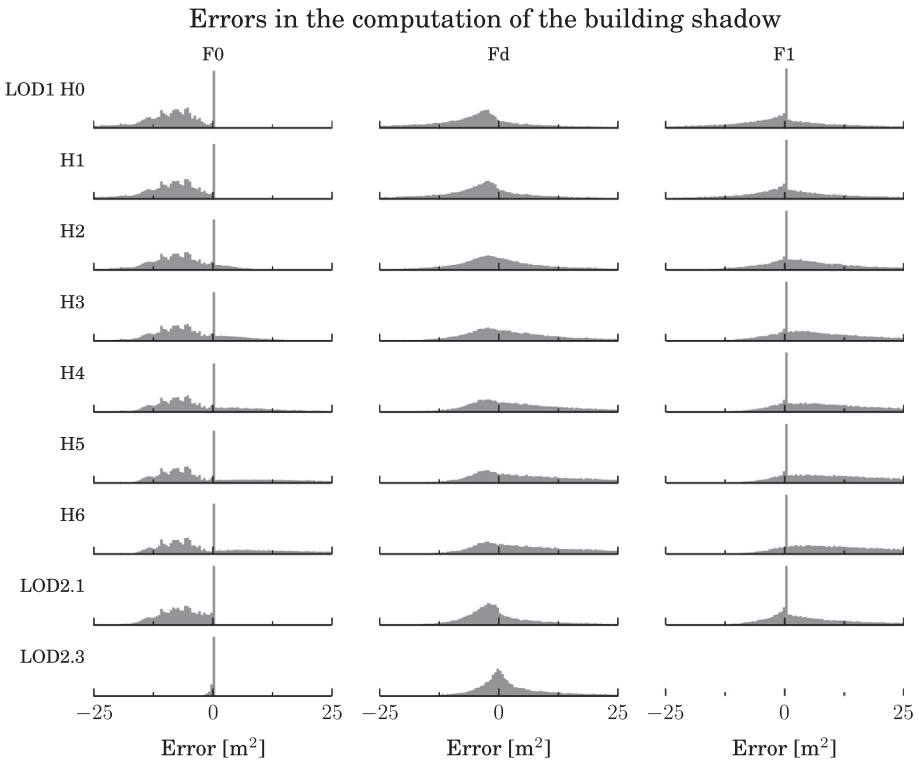

Fig. 9. Results of the third experiment involving the estimation of the area of the shadow cast on the ground.

5. Conclusions and recommendations

In this paper we have researched geometric references in 3D building models, an important but frequently overlooked concept of the multiple representations of 3D city models that are of the same level of detail. We have examined geometric references in LOD1 and LOD2 models that appear frequently in practice, and we have performed experiments on data produced with a procedural modelling engine that generates 3D building models according to a large number of references. The experiments, performed on three use cases, have shown that there may be substantial discrepancies between models of different geometric references. This finding may also imply that there is no such thing as a general purpose 3D city model, since each use case prefers a model with a particular geometric reference. Therefore, when acquiring a 3D city model, the choice of the geometric reference should be driven by the intended use of the models. Furthermore, when dealing with multiple applications, one should accept uncertainty and the fact that the model will likely not be equally suitable for all applications.

An important and unexpected result is that the geometric reference may have a higher influence than the granularity (LOD) of the model: a coarse model acquired with a favourable geometric reference may yield a more accurate result than a finer model acquired with an adverse geometric reference.

Finally, in this section we give recommendations related to the adoption and utilisation of geometric references, and discuss a few important points.

5.1. Extension of the INSPIRE Building model

The INSPIRE Building model provides extensive metadata for the vertical and horizontal geometric references, but our research has shown that they are insufficient. We propose the following:

1. Supplementing the standard with additional references found in our research (Section 3).
2. Eliminating the ambiguous reference `generalroof` which indicates that the vertical reference may represent any point of the roof.
3. Enabling additional metadata on the references. For instance, in the case of the horizontal reference Fd, we propose enabling the notation of the offset; and in case of the reference Hx, we deem that it would be beneficial to state the lineage of the data that is used to derive the extruded models. This is especially beneficial for the increasing number of models derived by extruding footprints coupled with various information from cadastral data sets.

5.2. Extension of CityGML

CityGML is a common schema to store and exchange 3D city models, however, it does not provide a mechanism to store the geometric reference metadata, resulting in uncertainty and unknown lineage of the models. Therefore, we propose to extend the standard with INSPIRE metadata, and we have submitted a change request to the OGC to regard these geometric references.

However, instead of extending the schema, which is somewhat covered by the research of Gröger and Plümer (2013) and Biljecki et al. (2014b), we focus on two points of discussion that can aid the developers of the standard:

5.2.1. Cardinality of the representations

The current version of the CityGML standard does not support storing multiple representations of the same LOD. Consequently, it is not possible to store two LOD1 models with different geometric variants. We encourage the developers of the standard to take this into account, since each representation provides a different value for a spatial analysis, hence, enabling the possibility of storing multiple models of different GRs might enable practitioners to switch the GRs and select the most suitable one.

5.2.2. Granularity of the metadata

Nowadays, most of 3D city models are acquired with a consistent workflow, i.e. a city is surveyed by one party using one acquisition approach. This results in the geometric reference of buildings to be homogeneous across a data set.

However, an increasing number of 3D GIS data sets contains models of heterogeneous lineage, e.g. Over et al. (2010), Goetz and Zipf (2012), and Goetz (2013). In contrast to most models, this approach potentially results in different geometric references in the data set. For this reason, we argue that it is essential to provide the metadata on the building level, rather than on the data set level.

5.3. Integration in quality control procedures

The geometric reference is usually not considered in spatial data quality documents, e.g. ISO 19157 (ISO, 2013). We recommend the developers of quality standards to regard this important concept, by enabling the assessment of the geometric reference in the quality procedures, e.g. to express that the geometric reference in the data set does not correspond to the one noted in the metadata.

5.4. Production of an enhanced LOD2

Our experiments have shown that LOD2.3—the enhanced version of the LOD2—which contains explicitly modelled roof overhangs, may bring an improvement in accuracy and performance over the "usual" simple LOD2. Such models are not complex to acquire if terrestrial and airborne observations are available, hence, we encourage practitioners to consider this model in their production workflows.

Acknowledgements

We appreciate the information obtained from institutions and companies about their modelling practices which have served as input for this research. We gratefully acknowledge the comments by the anonymous reviewers. Furthermore, we thank Safe Software Inc. for providing us with a licence for FME.

This research is supported by the Dutch Technology Foundation STW, which is part of the Netherlands Organisation for Scientific Research (NWO), and which is partly funded by the Ministry of Economic Affairs (project code: 11300).

References

AdV, 2011. Produktstandard für 3D-Gebäudemodelle. Arbeitsgemeinschaft der Vermessungsverwaltungen der Länder der Bundesrepublik Deutschland (Working Committee of the Surveying Authorities of the States of the Federal Republic of Germany). Available online at <http://www.adv-online.de> (last accessed on 12 February 2016).

AdV, 2013. Modellierungsbeispiele für 3D-Gebäudemodelle. Arbeitsgemeinschaft der Vermessungsverwaltungen der Länder der Bundesrepublik Deutschland (Working Committee of the Surveying Authorities of the States of the Federal Republic of Germany). Available online at <http://www.adv-online.de> (last accessed on 12 February 2016).

Ahmed, F.C., Sekar, S.P., 2015. Using three-dimensional volumetric analysis in everyday urban planning processes. Appl. Spatial Anal. Policy 8, 393–408.

Alam, N., Coors, V., Zlatanova, S., 2013. Detecting shadow for direct radiation using CityGML models for photovoltaic potentiality analysis. In: Ellul, C., Zlatanova, S., Rumor, M., Laurini, R. (Eds.), Urban and Regional Data Management. CRC Press, London, UK, pp. 191–196.

Arefi, H., Engels, J., Hahn, M., Mayer, H., 2008. Levels of detail in 3D building reconstruction from LiDAR data. Int. Arch. Photogramm. Rem. Sens. Spatial Inf. Sci. XXXVII-B3b, 485–490.

Aringer, K., Roschlaub, R., 2014. Bavarian 3D building model and update concept based on LiDAR, image matching and cadastre information. In: Innovations in 3D Geo-Information Sciences. Springer International Publishing, pp. 143–157.

Arroyo Ohori, K., Ledoux, H., Biljecki, F., Stoter, J., 2015a. Modeling a 3D city model and its levels of detail as a true 4D model. ISPRS Int. J. Geo-Inform. 4, 1055–1075.

Arroyo Ohori, K., Ledoux, H., Stoter, J., 2015b. A dimension-independent extrusion algorithm using generalised maps. Int. J. Geogr. Inform. Sci. 29, 1166–1186.

Bahu, J.M., Koch, A., Kremers, E., Murshed, S.M., 2015. Towards a 3D spatial urban energy modelling approach. Int. J. 3-D Inform. Model. 3, 1–16.

Bajsanski, I., Stojakovic, V., Jovanovic, M., 2016. Effect of tree location on mitigating parking lot insolation. Comput. Environ. Urban Syst. 56, 59–67.

Becker, S., 2009. Generation and application of rules for quality dependent façade reconstruction. ISPRS J. Photogramm. Rem. Sens. 64, 640–653.

Benner, J., Geiger, A., Gröger, G., Häfele, K.H., Löwner, M.O., 2013. Enhanced LOD concepts for virtual 3D city models. ISPRS Ann. Photogramm. Rem. Sens. Spatial Inf. Sci. II-2/W1, 51–61.

Biljecki, F., Heuvelink, G.B.M., Ledoux, H., Stoter, J., 2015a. Propagation of positional error in 3D GIS: estimation of the solar irradiation of building roofs. Int. J. Geogr. Inform. Sci. 29, 2269–2294.

Biljecki, F., Ledoux, H., Stoter, J., 2014a. Error propagation in the computation of volumes in 3D city models with the Monte Carlo method. ISPRS Ann. Photogramm. Rem. Sens. Spatial Inf. Sci. II-2, 31–39.

Biljecki, F., Ledoux, H., Stoter, J., 2014b. Height references of CityGML LOD1 buildings and their influence on applications. In: Breunig, M., Mulhim, A.D., Butwilowski, E., Kuper, P.V., Benner, J., Häfele, K.H. (Eds.), Proceedings of the 9th 3DGeoInfo Conference 2014, Dubai, UAE.

Biljecki, F., Ledoux, H., Stoter, J., 2015b. Improving the consistency of multi-LOD CityGML datasets by removing redundancy. In: Breunig, M., Mulhim, A.D., Butwilowski, E., Kuper, P.V., Benner, J., Häfele, K.H. (Eds.), 3D Geoinformation Science. Springer International Publishing, pp. 1–17.

Biljecki, F., Ledoux, H., Stoter, J., 2016. An improved LOD specification for 3D building models. Comput. Environ. Urban Syst. (in preparation)

Biljecki, F., Ledoux, H., Stoter, J., Zhao, J., 2014c. Formalisation of the level of detail in 3D city modelling. Comput. Environ. Urban Syst. 48, 1–15.

Biljecki, F., Stoter, J., Ledoux, H., Zlatanova, S., Çöltekin, A., 2015c. Applications of 3D city models: state of the art review. ISPRS Int. J. Geo-Inform. 4, 2842–2889.

Boeters, R., Arroyo Ohori, K., Biljecki, F., Zlatanova, S., 2015. Automatically enhancing CityGML LOD2 models with a corresponding indoor geometry. Int. J. Geogr. Inform. Sci. 29, 2248–2268.

Brasebin, M., Perret, J., Mustière, S., Weber, C., 2012. Measuring the impact of 3D data geometric modeling on spatial analysis: illustration with Skyview factor. In: Leduc, T., Moreau, G., Billen, R. (Eds.), Usage, Usability, and Utility of 3D City Models – European COST Action TU0801, EDP Sciences, Nantes, France, pp. (02001)1–16.

Brasebin, M., Perret, J., Mustiere, S., Weber, C., 2016. A generic model to exploit urban regulation knowledge. ISPRS Int. J. Geo-Inform. 5, 14.

van den Brink, L., Stoter, J., Zlatanova, S., 2013. Establishing a national standard for 3D topographic data compliant to CityGML. Int. J. Geogr. Inform. Sci. 27, 92–113.

Burnicki, A.C., Brown, D.G., Goovaerts, P., 2007. Simulating error propagation in land-cover change analysis: the implications of temporal dependence. Comput. Environ. Urban Syst. 31, 282–302.

Chwieduk, D.A., 2009. Recommendation on modelling of solar energy incident on a building envelope. Renew. Energy 34, 736–741.

Commandeur, T., 2012. Footprint Decomposition Combined with Point Cloud Segmentation for Producing Valid 3D Models. Master's thesis. Delft University of Technology.

Coors, V., 2003. 3D-GIS in networking environments. Comput. Environ. Urban Syst. 27, 345–357.

Czerwinski, A., Sandmann, S., Elke, S.M., Plümer, L., 2007. Sustainable SDI for EU noise mapping in NRW – best practice for INSPIRE. Int. J. Spatial Data Infrastruct. Res. 2, 1–18.

Demir, N., Baltsavias, E.P., 2012. Automated modeling of 3D building roofs using image and LiDAR data. ISPRS Ann. Photogramm. Rem. Sens. Spatial Inf. Sci. I-4, 35–40.

Diakité, A.A., Damiand, G., Van Maercke, D., 2014. Topological reconstruction of complex 3D buildings and automatic extraction of levels of detail. In: Besuievsky, G., Tourre, V. (Eds.), Eurographics Workshop on Urban Data Modelling and Visualisation, Strasbourg, France, pp. 25–30.

Dong, P., Ramesh, S., Nepali, A., 2010. Evaluation of small-area population estimation using LiDAR, Landsat TM and parcel data. Int. J. Rem. Sens. 31, 5571–5586.

Eicker, U., Nouvel, R., Duminil, E., Coors, V., 2014. Assessing passive and active solar energy resources in cities using 3D city models. Energy Proc. 57, 896–905.

El-Mekawy, M., Östman, A., Shahzad, K., 2011. Towards interoperating CityGML and IFC building models: a unified model based approach. In: Kolbe, T.H., König, G., Nagel, C. (Eds.), Advances in 3D Geo-Information Sciences. Springer Berlin Heidelberg, Berlin, Heidelberg, pp. 73–93.

Fisher-Gewirtzman, D., Shashkov, A., Doytsher, Y., 2013. Voxel based volumetric visibility analysis of urban environments. Surv. Rev. 45, 451–461.

Fogl, M., Moudrý, V., 2016. Influence of vegetation canopies on solar potential in urban environments. Appl. Geogr. 66, 73–80.

Forberg, A., 2007. Generalization of 3D building data based on a scale-space approach. ISPRS J. Photogramm. Rem. Sens. 62, 104–111.

Franić, S., Bačić-Deprato, I., Novaković, I., 2009. 3D model and a scale model of the City of Zagreb. Int. Arch. Photogramm. Rem. Sens. Spatial Inf. Sci. XXXVIII-2/W11, 1–7.

Glander, T., Döllner, J., 2009. Abstract representations for interactive visualization of virtual 3D city models. Comput. Environ. Urban Syst. 33, 375–387.

Goetz, M., 2013. Towards generating highly detailed 3D CityGML models from OpenStreetMap. Int. J. Geogr. Inform. Sci. 27, 845–865.
Goetz, M., Zipf, A., 2012. Towards defining a framework for the automatic derivation of 3D CityGML models from volunteered geographic information. Int. J. 3-D Inform. Model. 1, 1–16.
Gröger, G., Plümer, L., 2012. CityGML – interoperable semantic 3D city models. ISPRS J. Photogramm. Rem. Sens. 71, 12–33.
Gröger, G., Plümer, L., 2013. The interoperable building model of the European union. In: Abdul-Rahman, A., Boguslawski, P., Anton, F., Said, M.N., Omar, K.M. (Eds.), Geoinformation for Informed Decisions. Springer International Publishing, pp. 1–17.
Guercke, R., Götzelmann, T., Brenner, C., Sester, M., 2011. Aggregation of LoD 1 building models as an optimization problem. ISPRS J. Photogramm. Rem. Sens. 66, 209–222.
Haala, N., Kada, M., 2010. An update on automatic 3D building reconstruction. ISPRS J. Photogramm. Rem. Sens. 65, 570–580.
He, S., Besuievsky, G., Tourre, V., Patow, G., Moreau, G., 2012a. All range and heterogeneous multi-scale 3D city models. In: Leduc, T., Moreau, G., Billen, R. (Eds.), Usage, Usability, and Utility of 3D City Models – European COST Action TU0801, EDP Sciences, Nantes, France.
He, S., Moreau, G., Martin, J.Y., 2013. Footprint-based generalization of 3D building groups at medium level of detail for multi-scale urban visualization. Int. J. Adv. Softw. 5, 378–388.
He, Y., Zhang, C., Awrangjeb, M., Fraser, C.S., 2012b. Automated reconstruction of walls from airborne LiDAR data for complete 3D building modelling. Int. Arch. Photogramm. Rem. Sens. Spatial Inf. Sci. XXXIX-B3, 115–120.
Helbich, M., Jochem, A., Mücke, W., Höfle, B., 2013. Boosting the predictive accuracy of urban hedonic house price models through airborne laser scanning. Comput. Environ. Urban Syst. 39, 81–92.
Herbert, G., Chen, X., 2015. A comparison of usefulness of 2D and 3D representations of urban planning. Cartogr. Geogr. Inform. Sci. 42, 22–32.
Hermosilla, T., Ruiz, L.A., Recio, J.A., Cambra-López, M., 2012. Assessing contextual descriptive features for plot-based classification of urban areas. Landscape Urban Plan. 106, 124–137.
van der Hoeven, F., Wandl, A., 2015. Hotterdam: How Space is Making Rotterdam Warmer, How this Affects the Health of Its Inhabitants, and What can be Done About It. TU Delft.
Hofierka, J., Zlocha, M., 2012. A new 3-D solar radiation model for 3-D city models. Trans. GIS 16, 681–690.
Hsieh, C.M., Aramaki, T., Hanaki, K., 2011. Managing heat rejected from air conditioning systems to save energy and improve the microclimates of residential buildings. Comput. Environ. Urban Syst. 35, 358–367.
INSPIRE Thematic Working Group Buildings, 2013. D2.8.III.2 INSPIRE Data Specification on Buildings – Technical Guidelines.
ISO, 2013. ISO 19157:2013 – Geographic Information – Data Quality.
Johnson, G.T., Watson, I.D., 1984. The determination of view-factors in urban canyons. J. Clim. Appl. Meteorol. 23, 329–335.
Kaden, R., Kolbe, T.H., 2013. City-wide total energy demand estimation of buildings using semantic 3D city models and statistical data. ISPRS Ann. Photogramm. Rem. Sens. Spatial Inf. Sci. II-2/W1, 163–171.
Kaden, R., Kolbe, T.H., 2014. Simulation-based total energy demand estimation of buildings using semantic 3D city models. Int. J. 3-D Inform. Model. 3, 35–53.
Kolbe, T.H., 2009. Representing and exchanging 3D city models with CityGML. In: Zlatanova, S., Lee, J. (Eds.), 3D Geo-Information Sciences. Springer, Berlin Heidelberg, pp. 15–31.
Kolbe, T.H., Burger, B., Cantzler, B., 2015. CityGML goes to Broadway. In: Photogrammetric Week '15, Stuttgart, Germany, pp. 343–356.
Kwan, M.P., 2000. Interactive geovisualization of activity-travel patterns using three-dimensional geographical information systems: a methodological exploration with a large data set. Transport. Res. Part C – Emer. Technol. 8, 185–203.
Ledoux, H., Meijers, M., 2011. Topologically consistent 3D city models obtained by extrusion. Int. J. Geogr. Inform. Sci. 25, 557–574.
Li, Q., Sun, X., Yang, B., Jiang, S., 2013. Geometric structure simplification of 3D building models. ISPRS J. Photogramm. Rem. Sens. 84, 100–113.
Li, Y., Brimicombe, A.J., Ralphs, M.P., 2000. Spatial data quality and sensitivity analysis in GIS and environmental modelling: the case of coastal oil spills. Comput. Environ. Urban Syst. 24, 95–108.
Löwner, M.O., Benner, J., Gröger, G., Häfele, K.H., 2013. New concepts for structuring 3D city models – an extended level of detail concept for CityGML buildings. In: Murgante, B., Misra, S., Carlini, M., Torre, C.M., Nguyen, H.Q., Taniar, D., Apduhan, B.O., Gervasi, O. (Eds.), Spatial Information Theory. Cognitive and Computational Foundations of Geographic Information Science. Springer, Berlin Heidelberg, pp. 466–480.
Lwin, K., Murayama, Y., 2009. A GIS approach to estimation of building population for micro-spatial analysis. Trans. GIS 13, 401–414.
Mao, B., Harrie, L., Ban, Y., 2012. Detection and typification of linear structures for dynamic visualization of 3D city models. Comput. Environ. Urban Syst. 36, 233–244.
Maragkogiannis, K., Kolokotsa, D., Maravelakis, E., Konstantaras, A., 2014. Combining terrestrial laser scanning and computational fluid dynamics for the study of the urban thermal environment. Sustain. Cities Soc. 13, 207–216.
Meinel, G., Hecht, R., Herold, H., 2009. Analyzing building stock using topographic maps and GIS. Build. Res. Inform. 37, 468–482.
Morello, E., Ratti, C., 2009. Sunscapes: 'Solar envelopes' and the analysis of urban DEMs. Comput. Environ. Urban Syst. 33, 26–34.
Musialski, P., Wonka, P., Aliaga, D.G., Wimmer, M., van Gool, L., Purgathofer, W., 2013. A survey of urban reconstruction. Comput. Graph. Forum 32, 146–177.
Nguyen, H.T., Pearce, J.M., 2012. Incorporating shading losses in solar photovoltaic potential assessment at the municipal scale. Sol. Energy 86, 1245–1260.
Nouvel, R., Schulte, C., Eicker, U., Pietruschka, D., Coors, V., 2013. CityGML-based 3D city model for energy diagnostics and urban energy policy support. In: Proceedings of BS2013: 13th Conference of International Building Performance Simulation Association, Chambéry, France, pp. 218–225.
Novaković, I., 2011. 3D model of Zagreb. GIM Int. 25, 25–29.
Open Geospatial Consortium, 2012. OGC City Geography Markup Language (CityGML) Encoding Standard 2.0.0. Technical Report.
Ordnance Survey, 2014. OS MasterMap Topography Layer. User Guide and Technical Specification, 1.12 ed.
Oude Elberink, S., 2008. Problems in automated building reconstruction based on dense airborne laser scanning data. Int. Arch. Photogramm. Rem. Sens. Spatial Inf. Sci. XXXVII, 93–98.
Oude Elberink, S., 2010. Acquisition of 3D Topography: Automated 3D Road and Building Reconstruction using Airborne Laser Scanner Data and Topographic Maps. Ph.D. thesis. ITC, University of Twente. Enschede, the Netherlands.
Oude Elberink, S., Stoter, J., Ledoux, H., Commandeur, T., 2013. Generation and dissemination of a national virtual 3D city and landscape model for the Netherlands. Photogramm. Eng. Rem. Sens. 79, 147–158.
Over, M., Schilling, A., Neubauer, S., Zipf, A., 2010. Generating web-based 3D city models from OpenStreetMap: the current situation in Germany. Comput. Environ. Urban Syst. 34, 496–507.
Pedrinis, F., Gesquière, G., 2016. Reconstructing 3D building models with the 2D cadastre for semantic enhancement. In: Abdul-Rahman, A. (Ed.), Advances in 3D Geoinformation. Springer International Publishing.
Perez, D., Kämpf, J.H., Scartezzini, J.L., 2013. Urban area energy flow microsimulation for planning support: a calibration and verification study. Int. J. Adv. Syst. Meas. 6, 260–271.
Previtali, M., Barazzetti, L., Brumana, R., Cuca, B., Oreni, D., Roncoroni, F., Scaioni, M., 2014. Automatic façade modelling using point cloud data for energy-efficient retrofitting. Appl. Geomatics 6, 95–113.
Ranjbar, H.R., Gharagozlou, A.R., Nejad, A.R.V., 2012. 3D analysis and investigation of traffic noise impact from Hemmat highway located in tehran on buildings and surrounding areas. J. Geogr. Inform. Syst. 4, 322–334.
Rottensteiner, F., 2003. Automatic generation of high-quality building models from lidar data. IEEE Comput. Graph. Appl. 23, 42–50.
Sargent, I., Holland, D., Harding, J., 2015. The building blocks of user-focused 3D city models. ISPRS Int. J. Geo-Inform. 4, 2890–2904.
Schwalbe, E., Maas, H.G., Seidel, F., 2005. 3D building model generation from airborne laser scanner data using 2D GIS data and orthogonal point cloud projections. Int. Arch. Photogramm. Rem. Sens. Spatial Inf. Sci. XXXVI-3/W19, 209–214.
Sirmacek, B., Taubenbock, H., Reinartz, P., Ehlers, M., 2012. Performance evaluation for 3-D city model generation of six different DSMs from air- and spaceborne sensors. IEEE J. Sel. Top. Appl. Earth Obs. Rem. Sens. 5, 59–70.
Sridharan, H., Qiu, F., 2013. A spatially disaggregated areal interpolation model using light detection and ranging-derived building volumes. Geogr. Anal. 45, 238–258.
Stadler, A., Kolbe, T.H., 2007. Spatio-semantic coherence in the integration of 3D city models. Int. Arch. Photogramm. Rem. Sens. Spatial Inf. Sci. XXXVI-2/C43, 8.
Steuer, H., Machl, T., Sindram, M., Liebel, L., Kolbe, T.H., 2015. Voluminator—approximating the volume of 3D buildings to overcome topological errors. In: AGILE 2015. Springer International Publishing, pp. 343–362.
Stoter, J., de Kluijver, H., Kurakula, V., 2008. 3D noise mapping in urban areas. Int. J. Geogr. Inform. Sci. 22, 907–924.
Stoter, J., Roensdorf, C., Home, R., Capstick, D., Streilein, A., Kellenberger, T., Bayers, E., Kane, P., Dorsch, J., Woźniak, P., Lysell, G., Lithen, T., Bucher, B., Paparoditis, N., Ilves, R., 2015. 3D modelling with national coverage: bridging the gap between research and practice. In: Advances in 3D Geo-Information Sciences. Springer International Publishing, Cham, Switzerland, pp. 207–225.
Stoter, J., Vosselman, G., Dahmen, C., Oude Elberink, S., Ledoux, H., 2014. CityGML implementation specifications for a countrywide 3D data set: the case of the Netherlands. Photogramm. Eng. Rem. Sens. 80, 13–21.
Strzalka, A., Alam, N., Duminil, E., Coors, V., Eicker, U., 2012. Large scale integration of photovoltaics in cities. Appl. Energy 93, 413–421.
Strzalka, A., Bogdahn, J., Coors, V., Eicker, U., 2011. 3D city modeling for urban scale heating energy demand forecasting. HVAC&R Res. 17, 526–539.
Strzalka, A., Eicker, U., Coors, V., Schumacher, J., 2010. Modeling energy demand for heating at city scale. In: Proceedings of SimBuild 2010, 4th National Conference of IBPSA-USA, New York City, NY, United States, pp. 358–364.
Suveg, I., Vosselman, G., 2004. Reconstruction of 3D building models from aerial images and maps. ISPRS J. Photogramm. Rem. Sens. 58, 202–224.
SwissTopo, 2010. SwissBUILDINGS3D 1.0. Vereinfachte 3D-Gebäude der Schweiz. Product Brochure and Documentation.
Tomljenovic, I., Höfle, B., Tiede, D., Blaschke, T., 2015. Building extraction from airborne laser scanning data: an analysis of the state of the art. Rem. Sens. 7, 3826–3862.
Ural, S., Hussain, E., Shan, J., 2011. Building population mapping with aerial imagery and GIS data. Int. J. Appl. Earth Obs. Geoinf. 13, 841–852.
Verdie, Y., Lafarge, F., Alliez, P., 2015. LOD generation for urban scenes. ACM Trans. Graph. 34, 1–14.

Wang, L., Groves, P.D., Ziebart, M.K., 2013. GNSS shadow matching: improving urban positioning accuracy using a 3D city model with optimized visibility scoring scheme. Navigation 60, 195–207.
Xiong, B., Jancosek, M., Oude Elberink, S., Vosselman, G., 2015. Flexible building primitives for 3D building modeling. ISPRS J. Photogramm. Rem. Sens. 101, 275–290.
Yaagoubi, R., Yarmani, M., Kamel, A., Khemiri, W., 2015. HybVOR: a voronoi-based 3D GIS approach for camera surveillance network placement. ISPRS Int. J. Geo-Inform. 4, 754–782.
Yang, P.P., Putra, S.Y., Li, W., 2007. Viewsphere: a GIS-based 3D visibility analysis for urban design evaluation. Environ. Plan. B: Plan. Des. 34, 971.
Zhang, K., Yan, J., Chen, S.C., 2006. Automatic construction of building footprints from airborne LIDAR data. IEEE Trans. Geosci. Rem. Sens. 44, 2523–2533.
Zhao, J., Zhu, Q., Du, Z., Feng, T., Zhang, Y., 2012. Mathematical morphology-based generalization of complex 3D building models incorporating semantic relationships. ISPRS J. Photogramm. Rem. Sens. 68, 95–111.